Luminescence Characteristics of LaAlO₃:Eu³⁺ Obtained by Modified Pechini's Method

Alfredo Morales Hernández[1,2]*, Mayra A. de León Alfaro[2], Antonio Barrera Villatoro[1,2], Ciro Falcony[3], Teodoro Rivera Montalvo[2], Juan Zarate Medina[1]

[1]Instituto de Investigaciones en Metalurgia y Materiales, Universidad Michoacana de San Nicolás de Hidalgo, Morelia, México
[2]Instituto Politécnico Nacional, Centro de Investigación en Ciencia Aplicada y Tecnología Avanzada, Ciudad de México, México
[3]Centro de Investigación y de Estudios Avanzados del Instituto Politécnico Nacional, Ciudad de México, México
Email: *feyo_yo@hotmail.com

Abstract

The aim of the present work was to investigate the luminescent properties of europium-doped lanthanum aluminate (LaAlO₃) powder prepared by Modified Pechini (MP) method. Samples were prepared at different Eu³⁺ concentrations and calcined at 1600°C. Structural and morphology characterizations were obtained by X-ray diffraction (XRD), scanning electron microscopy (SEM), and transmission electron microscope (TEM). Luminescent properties were analyzed by photoluminescence (PL) and thermoluminescent phenomena. The XRD pattern shows pure lanthanum aluminate oxide LaAlO₃ with a rhombohedral structure. Photoluminescence studies of the powders was related to $4f \rightarrow 4f$ ($^5D_0 \rightarrow {}^7F_i$) (i = 1, 2, 3, 4) transitions of Eu³⁺ ion, the most intense emission of Eu³⁺ in LaAlO₃ was registered for the transition $^5D_0 \rightarrow {}^7F_1$, for 5% of Eu³⁺. The recorded TL glow curves of excited samples showed a main TL peak, the main peak appeared its maximum as a function of excitation energy. The investigation demonstrates that polycrystalline LaAlO₃:Eu³⁺ powders calcined at 1600°C have interesting luminescent characteristics.

Keywords

Modified Pechini Method, LaAlO₃:Eu³⁺, Photoluminescence, Thermoluminescence

1. Introduction

Luminescent materials have been widely studied and applied in a number of applications including solid-state lighting, display, photovoltaics and detectors. Luminescent materials can be found in a broad range of everyday applications such as cathode ray tubes (CRTs), projection televisions, fluorescent lamps,

X-ray detectors, solid state lighting, sensors, and displays [1]. Phosphors are luminescent materials that efficiently emit light upon electromagnetic or particle excitation. Light emission can be observed easily in polycrystalline materials when these are subjected to an exciting agent (ionizing radiation) and subsequently analyzed by the stimulated luminescence phenomena [2]. The energy of the excited photons is absorbed and dispersed through the materials in the form of energetic electrons and holes [1] [2]. Eventually, these high-energy charge carriers relax toward the electronic ground state by either a radiative relaxation resulting in luminescence. Consequently, research and development on luminescent materials has resulted in synthesis and testing of thousands of phosphors. An increasing important application of luminescent material is for down conversion phosphor to create white light emitting diodes (W-LEDs) [3] [4]. Luminescence in rare-earth elements (REE) doped luminescent materials is a process by which ultraviolet light converted into visible light due to their sharp 4f-intra shell transitions [4] [5] [6]. Among these ions, europium is the most widely used activator and has been used in phosphor materials for an efficient red and blue emission. The europium emission in the phosphor material is strongly dependent on the host lattice and it is possible to obtain different colors from blue to red. Optical properties of the trivalent europium (Eu^{3+}) doped crystals and several research groups have studied glasses. They have investigated Eu^{3+} emission in borates, oxides, silicates, phosphates, sulfates and fluorides [4] [6] [7] [8] [9] [10], etc. The small amount of intentionally doped europium in the host matrix is essential for the development of photoluminescent devices. These materials find their applications in lighting, information display, and optoelectronics technology. The photoluminescence properties of RE-doped compounds not only depend on the composition and local structure of the host but also affected by its crystal size and morphology. The effect of the impurities in the matrix [11] [12] [13] [14] as well as in alkaline earth aluminates doped with RE^{3+} ions (R: rare earth) have been the subject of investigation as luminescent materials [15]. The emission of $LaAlO_3$:Eu^{3+} nanocrystals has been investigated and mechanism of luminescence has been proposed in literature by some investigators [16]. Few published papers report on the synthesis [17] [18], optical properties [19] and ultraviolet stimulated emission [20] of the RE^{3+}- doped $LaAlO_3$ nanocrystals. Vijay *et al* reported [21] the TL glow curve gamma irradiated of $LaAlO_3$ doped with europium. But in the literature it was noticed that there are no information of lanthanum aluminate doped with europium irradiated with X-ray beam. Historically, $LaAlO_3$ has been prepared by conventional solid-state reaction of Al_2O_3 and La_2O_3 in the temperature range 1500˚C - 1700˚C [22]. This conventional solid-state reaction process suffers from many inherent shortcomings, such as high reaction temperature, large particle size, limited chemical homogeneity and low sinterability. Other synthesis methods have been also developed to fabricate the inorganic functional materials, such as precipitation, combustion, and sol-gel processes [23] [24] [25] [26]. The last method so-called wet method, generally need long time to obtain nanosized

particles. Therefore, the aim of the present work was to synthesize Eu^{3+} doped $LaAlO_3$ powders using modified Pechini method and investigate its luminescent characteristics.

2. Experimental Details

Keeping in view, lanthanides and aluminates based phosphor as a new luminescent material in the field of optical devices; the following luminescent powders have been prepared by modified Pechini's (MP) method [27] [28] [29]. All chemical reagents were analytical grade and used without further purification. Stoichiometric quantity of solid mixture of $La(NO_3)_3 \cdot 6H_2O$, and $Al(NO_3)_3 \cdot 6H_2O$ were diluted in deionized water and Eu_2O_3 was well diluted in nitric acid solution. The Eu^{3+} concentration in the solution was in the range from 0.5 to 20 at %, with respect to the amount of lanthanum content, having been found that the optimal concentration correspond at 5 atomic percent in relation to lanthanum content. Hence, an aqueous solution of citric acid $HOC(COOH)(CH_2COOH)_2 \cdot H_2O$ and ethylene glycol $HOCH_2CH_2OH$ was added to the metal solution (citric acid: metal nitrates: ethylene glycol molar ratio = 2:1:2). The solution formed was evaporated in a YAMATO–ADL31 Spray Dryer device that in place give granulated white gel. Entrance temperature in spray dryer was 200°C and exit temperature from this was 90°C. The gel was kept on a plate and placed into an oven for its pre-annealed at 400°C this is in order to eliminate all organic components. Powders were submitted at different calcination processes in the range from 800°C up to 1600°C. The best thermoluminescent response was obtained for that samples calcined at 1600°C. Then, all powders were submitted at 1600°C for all characterization processes. X-ray diffraction (XRD) patterns of all samples were recorded on a SIEMMENS D5000 diffractometer with Cu $K\alpha$ radiation (1.54056 Å). The surface morphology was obtained using a scanning electron microscopy (SEM) Model No. JEOL, JSM-6400 instrument. The morphology of the samples was characterized by transmission electronic microscopy (TEM) (Tecnai F20). Photoluminescence (PL) measurements were performed with a UV-VIS FluoroMax-P Jobin Yvon Horiba spectrometer. 50 mg powder samples were pressed to obtain pellets and then exposed into a spectrometer. A Xenon arc lamp was used as a broadband excitation source and a double Czerny-turner monochromator was used to select the excitation wavelength for photoluminescence excitation. For high energy X-ray irradiation processes were done using an accelerator Elekta SYNERGY, with nominal energy of 6 MV using a radiation field size of 10×10 cm^2, at an absorbed dose of 1 Gy. For UV irradiation, the samples were individually exposed to UVR from a 150 W Xe arc lamp coupled to a monochromator for selecting the desired wavelength. Thermoluminescent (TL) signal was obtained using an analyzer Harshaw model 3500 connected to a PC in order to store and to analyze the glow curves, digitizing both TL and temperature signals by means of two channels of an RS232C interface. The linear heating rate of the TL analyzer was kept at 10°C/s for all the TL readings, which were made integrating the signal from 50°C up to 350°C. All TL measurements

were made in a nitrogen atmosphere in order to reduce the thermal noise from the heating planchet of the TL reader.

In this study to extract, the information about positions of the TL emission, peak shape method was employed. The method consists in the temperature at the maximum emission, T_M, the temperature on the ascending part of the peak, T_1, corresponding to the half peak intensity and the temperature on the descending part of the peak, T_2, and the half width parameters and the symmetry properties $\omega = T_2 - T_1, \delta = T_2 - T_M$ and $t = T_M - T_1$. The symmetry factor (μ_g) of the glow peak μ_g was obtained using Equation (1) from the peak shape parameters δ and ω.

$$\mu_g = \frac{\delta}{\omega} = \frac{T_2 - T_M}{T_2 - T_1} \tag{1}$$

Experimental kinetic parameters of Eu^{3+} doped $LaAlO_3$ powders were obtained exposing the powders contained into a cup with UV radiation at 230 nm at a dose of 10 mJ/cm^2. The same powders X-ray irradiated were used for kinetic parameters calculation. The activation energy (E) of the TL glow curve of LaAlO$_3$:Eu^{3+} was calculated using different equations expressed by peak shape method by mean of the second order kinetics proposed by Chen modified [30] [31] equation, and is given by:

Chen modified equation

$$E_\infty = c_\infty \frac{kT_M^2}{\infty} - b_\alpha 2kT_M \tag{2}$$

where α stands for τ, δ and ω respectively, c_α and b_α were obtained using the expressions given below:

$$c_\tau = 1.51 + 3.0 \left(\mu_g - 0.42 \right), b_\tau = 1.58 + 4.2 \left(\mu_g - 0.42 \right)$$
$$c_\delta = 0.976 + 7.3 \left(\mu_g - 0.42 \right), b_\delta = 0$$
$$c_\omega = 2.52 + 10.2 \left(\mu_g - 0.42 \right), b_\tau = 1$$

3. Results and Discussion

The X-ray diffraction patterns of europium trivalent doped LaALO$_3$ submitted at 1600˚C is shown in Figure 1. According to XRD analysis, a pure rhombohedral crystal phase of LaAlO$_3$ (PDF01-085-1071) with a perovskite structure is obtained at 1600˚C. The results of XRD measurements for doped (with 5% of Eu^{3+} ions) and, undoped LaAlO$_3$ powders show no significant alterations in the position peaks between undoped and Eu doped samples. The diffraction patterns for other dopant concentration are not included because XRD patterns were similar than those obtained for five percent doped samples. In the same figure it seems that the doping impurity does not influence the crystalline formation. Then, all diffraction peaks in these XRD patterns could be attributed to the rhombohedral structure of perovskite system with space group R-3m. X-ray diffraction patters of LaAlO$_3$ was similar than that reported by Rivera *et al.* [32].
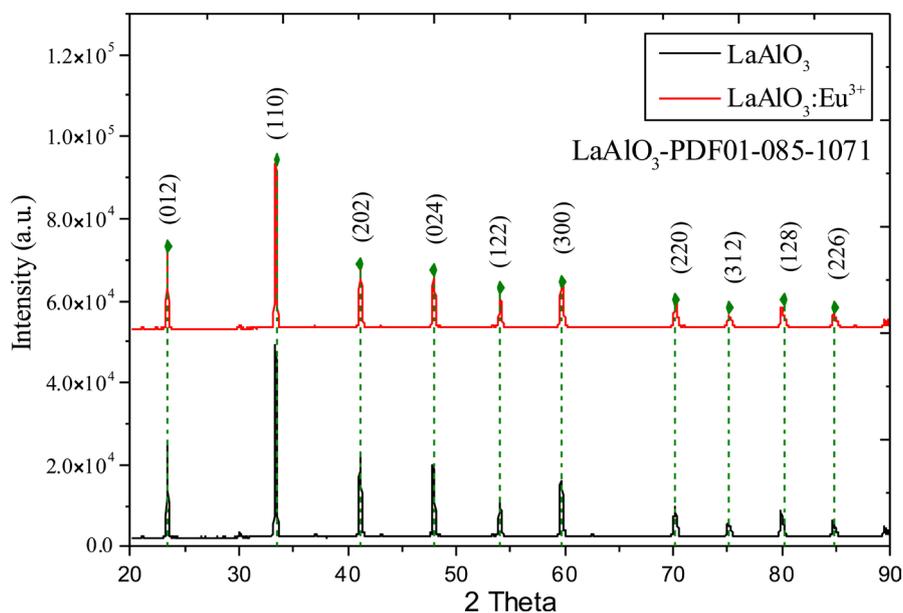
Figure 1. X-ray diffraction pattern of LaAlO$_3$:Eu^{3+} host lattice obtained at 1600°C.
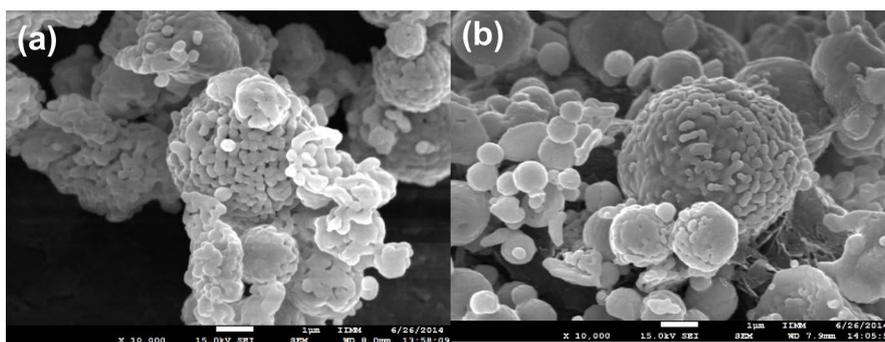
Figure 2. SEM micrographs of powders obtained at 1600°C of calcination temperature.

The SEM micrographs were obtained by JEOL JSM6300 scanning electron microscope. **Figure 2** exhibit surface morphologies of Eu^{3+} doped LaAlO$_3$ particles. The SEM images revealed that the crystallites have no uniform shapes and the sizes. As it can be seen, the powders are composed by crystals and exhibit the formation of aggregate among them. Spherical agglomerated within average range of 2 ± 0.5 um. The aggregation of powders, apparently, should result of the sintered density for LaAlO$_3$ materials made of these powders. Eu^{3+} doped powders submitted at 1600°C particles size could be show less compaction and less agglomeration particles formed by smaller particles than that obtained in the previous work, this is could be, the calcination processes was uploaded until 1600°C, meanwhile, in the previous work this was stopped at 1000°C and 1200°C.

Figure 3 illustrates the image obtained by a high resolution transmission electron microscope (HRTEM) images of europium trivalent-doped (La$_{0.95}$Eu$_{0.05}$AlO$_3$) powders calcined at 1600°C, showing that the powders are composed by crystalline particles and exhibit the uniform distribution of lattice planes. The HRTEM images of single samples having different distinct diameters are shown in **Figure 3**. The light field images in (**Figure 3(a)**), dark field in (**Figure 3(b)**), as it can be
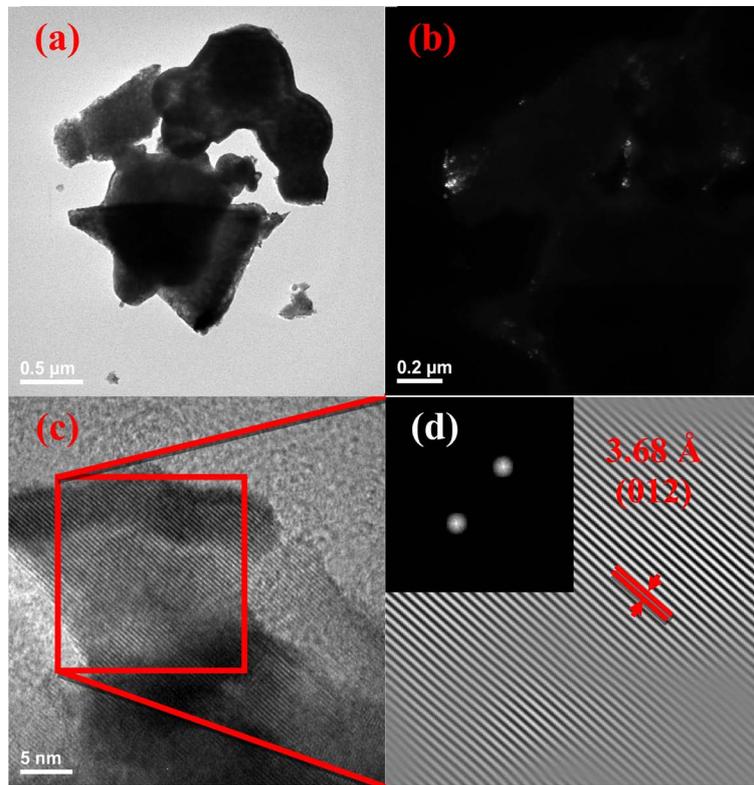
Figure 3. TEM micrographs of LaAlO$_3$:Eu^{3+} (5% Eu) powders synthesized at 1600°C: light field images in (a), dark field in (b), HRTEM image of LaAlO$_3$:Eu^{3+} (c) and HRTEM image (d) showing the plane (012) of rhombohedral phase.

seen in **Figure 3(a)**, an agglomerate of spherical morphology particles is observed in the light field image. In the dark field image (**Figure 3(b)**) the presence of small crystals on the surface of the agglomerate and (**Figure 3(c)**) in the high definition image shows the planes corresponding to the rhombohedral structure of the LAO phase belonging to the plane (012). The crystals have a crystalline structure with clearly interplanar distances between adjacent crystallographic planes for the LaAlO$_3$:Eu^{3+} polycrystalline powders. The lattice spacing of 3.68Å, seen in **Figure 3(d)**, corresponds to (012) growth directions of rhombohedral LaAlO$_3$.

The conventional luminescence spectra of the LaAlO$_3$:Eu^{3+} polycrystalline showed in **Figure 4**. The inset shows the corresponding excitation spectrum of LaAlO$_3$:Eu^{3+}, using a wavelength of 612 nm. The inset figure shows a maximum centered at 340 nm UV excited at room temperature. This spectrum was obtained with a fixed emission at λ = 613 nm. In this spectrum is possible to observe a broad excitation band centered at 340 nm can (could be related charge transfer transitions of 4f - 5d) be attributed to band-to-band transitions of the host lattice. For the present investigation, this excitation wavelength was selected for photoluminescent measurements. The obtained powders emitted both the orange and the red luminescence, which showed the activator Eu^{3+} has successfully entered in the LaAlO$_3$ lattice. As it can be two groups of sharp lines dominate seen PL emission spectra of Eu^{3+} at 594 and 619 nm. In previous works this
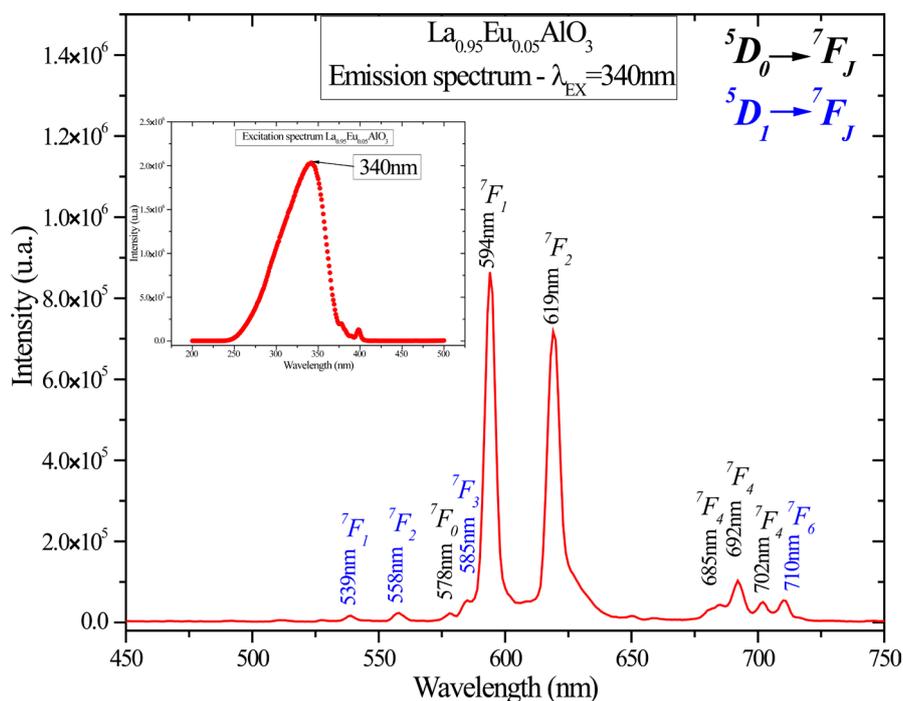
Figure 4. PL Emission spectra of Eu^{3+} 5% doped $LaAlO_3$ excited at 340 nm wavelength.

figure was published just to observe photoluminescent phenomena [32], but in the present work we try to explain the emission process. The emission observed at 594 nm corresponds to the magnetic dipole transition ($^5D_0 \to {}^7F_1$). Meanwhile the sharp line showed at 619 nm, which is in place of it is originated by the electric dipole ($^5D_0 \to {}^7F_2$) transition. The intensities of electric dipole transitions, in particular for J = 0 and for J = 2, are strongly sensitive to the rare earth surrounding environment, being absent in high symmetry sites, while the intensities of magnetic dipole transitions are independent of the environment. Therefore the ratio of intensities I ($^5D_0 \to {}^7F_2$)/I ($^5D_0 \to {}^7F_1$) is an indication of the symmetry around the rare-earth ion. The highest emission intensity was observed for $^5D_0 \to {}^7F_1$ transition, this is reverse than that expected. Dhahri and his group [17] reported that this transition emits a characteristic red light with number of narrow lines due to the intra-configurational 4f $\to$ 4f ($^5D_0 \to {}^7F_i$) (i = 1, 2, 3, 4) reported in the literature [21]. For our case, the $^5D_0 \to {}^7F_1$ transition is attributed as the responsible for the emission orange luminescence color, instead of the expected typical red color luminescence characteristic of Eu^{3+} ion as observed in other work [33]. A possible reason of emission orange color is a change in the local symmetry around of Eu^{3+} ion generating an inversion symmetric center in the host lattice. Europium trivalent emission can give information, on the local high symmetry around the rare-earth ion which responsible of highest emission intensity peak. Both these aspects are relevant for the physics of the system and for the potential applications. In addition, several lines were in place of are observed at around 700 nm, corresponding to the $^5D_0 \to {}^7F_4$ transition. The $^5D_0 \to {}^7F_1$ transitions are less common, are essentially attributed magnetic dipole transitions. The highest intensity peaks can allow evaluating its radiative lifetime
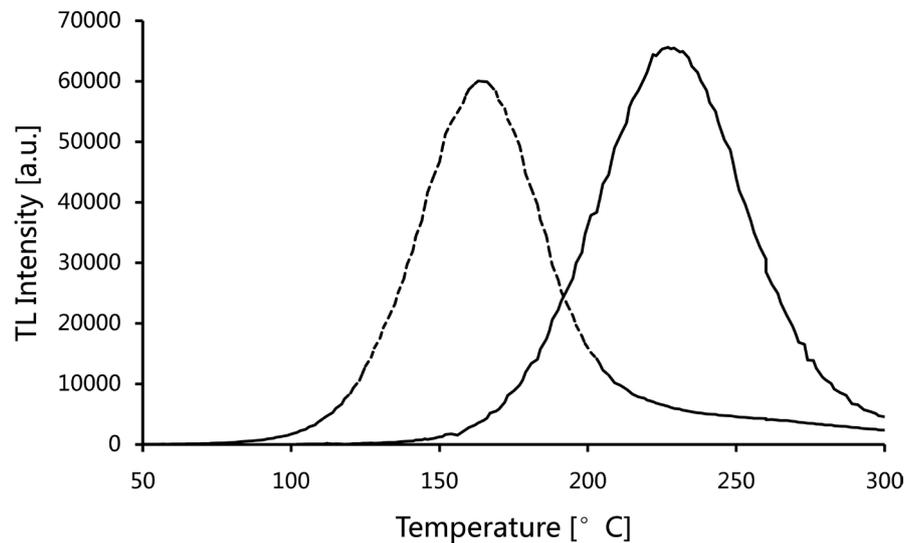
Figure 5. TL glow curve of: — LaAlO$_3$:Eu^{3+} powders (at UVR exposure). — LaAlO$_3$:Eu^{3+} induced by high energy X-ray beam.

(t_rad) by using a simple formula assuming that the energy of the $^5D_0 \rightarrow {}^7F_1$ transition and its oscillator strength are constant.

Figure 5 shows a corresponding typical TL glow curve of LaAlO$_3$:Eu^{3+} powders exposed to UV radiation (plotted by dashed line). TL response as a function of UV visible light wavelength was recorded from 200 nm to 400 nm having the highest peak centered at 230 nm. As it can be seen in the Figure 5, the TL glow curve of LaAlO$_3$:Eu^{3+} powders is constituted by a glow curve with a single peak centered in 165˚C when this is exposed at 230 nm UV wavelength. In this case UVR sensitivity of LaAlO$_3$:Eu^{3+} powders is about 10 times higher as compared to that obtained of TL response of undoped LaAlO$_3$ phosphor obtained under the same conditions processes. In the same Figure 5 can be seen a well defined TL glow curve of LaAlO$_3$:Eu^{3+} high energy X-ray irradiated. As it can be seen in this Figure 5, the TL glow curve of LaAlO$_3$:Eu^{3+} powders X-ray irradiated also exhibited by a single peak centered in 230˚C (plotted by full line). The TL glow curves UV irradiated as well as X-ray irradiated, both showed single glow peak this suggests that only one type of traps is being activated. The glow peak showed by full line is shifted toward high temperature, is due high energy X-ray perturbs high level energy of the crystal. High-energy X-ray beam allows releasing trapped electron deeper traps into the lattice and releasing them to produce broader wavelength light emission than that incident beam.

The opto-electronic properties of luminescent materials depend upon defects in crystal, chemical composition and doping of impurities. The study of thermoluminescence (TL) is very useful for determination of trapping parameter like activation energy, and frequency factor of luminescent materials. For the estimation of the activation energy and other parameters, most of the methods are basing on the mathematical approaches. For this investigation, the geometrical factor of the TL glow curve for the LaAlO$_3$:Eu^{3+} powders was calculated by using Equation (1). The geometrical factor value of the peak for sample UV irradiated

was equal to 0.49. Meanwhile, the geometrical factor for the sample but irradiated by high energy X-ray beam was 0.53, both geometrical factor values obey second order kinetic. Trap depth was found 1.08 ± 0.11 eV for samples exposed under UV radiation. Apparently, TL glow peak under UVR effects is similar than that obtained by X-ray irradiated samples. But a mathematical analysis concerning the thermoluminescent emission of light is the results of using lower energy excitation as well as UV energy, this processes just needs 1.08 eV to excite and moving charge carriers into lattice crystals until trap them into shallow traps. Meanwhile, samples irradiated under X-ray effect trap depth was 1.30 ± 0.09 eV. The mean activation energy of the same sample exhibited a glow peak with 1.30 eV as result of released deeper electron traps. From a theoretical point of view, the thermoluminescent phenomena describe electron traps directly connected to the band structure of solids and particularly to the effects of impurities and lattice irregularities. Then, it describes as centers that may occur when ions of either signs move away from their original sites, thus leaving vacancy states, able to interact with free charge carriers and to trap them. This indicates that Eu^{3+} ions in host lattice occupies an inversion center. Alternatively, ions can diffuse in interstitial positions and break locally the ideal lattice geometry; finally, impurity ions can perturb the lattice order, because of their sizes and valences, generally different from their neighbor ones. Therefore, these values reveal quite a complex configuration, and the experimental TL emission study can provide a satisfactory tool to get detailed information on its most meaningful parameters.

4. Conclusion

Eu^{3+} doped $LaAlO_3$ powders were successfully synthesized by the modified Pechini method, Pure $LaAlO_3$ phase was obtained at 1600°C. The XRD pattern shows pure perovskite oxide $LaAlO_3$ with a rhombohedral structure. Dopant (Eu^{3+}) ion concentration has no effect on the obtained X-ray diffractograms of $LaAlO_3:Eu^{3+}$. Photoluminescence (PL) emission was recorded under 340 nm excitation shows an intense emission peak at 594 nm along should be attributed to the magnetic transition with other emission peaks at 619, 692, 605 and 702 nm. $LaAlO_3:Eu^{3+}$ as luminescent material shows very high orange luminescence of nearly 594 nm, and this effect could be attributed a change in the local symmetry caused by Eu^{3+} ion, which is definitely a material for further investigation for its use in lighting applications. The TL glow curve for Eu^{3+} doped $LaAlO_3$ expressed second order kinetics. Trap depth was found to be in the range of 1.08 - 1.30 eV. These values suggest TL signal from samples exposed under UV radiation correspond to shallow traps which should be useful for this material as UV radiation monitor. Meanwhile, TL signal obtained from $LaAlO_3:Eu^{3+}$ under X-ray effect correspond to deep traps and suggests as a good material as ionizing radiation dosimeter.

Acknowledgements

177912, and CIC-UMSNH project..

References

[1] Dexter, D.L. (1953) A Theory of Sensitized Luminescence in Solids. *Journal of Chemistry and Physics*, **21**, 836-850. https://doi.org/10.1063/1.1699044

[2] DeLuca, J.A. (1980) An Introduction to Luminescence in Inorganic Solids. *Journal of Chemical in Education*, **57**, 541-545. https://doi.org/10.1021/ed057p541

[3] Jonscher, A.K. and de Polignac, A. (1984) The Time Dependence of Luminescence in Solids. *Journal of Physics C: Solid State Physics*, **17**, 6493-6520. https://doi.org/10.1088/0022-3719/17/35/018

[4] Phaomei, G., Singh, W.R., Singh, N.S. and Ningthoujam, R.S. (2013) Luminescence Properties of Ce^{3+} Co-Activated $LaPO_4$:Dy^{3+} Nanorods Prepared in Different Solvents and Tunable Blue to White Light Emission from Eu^{3+} Co-Activated $LaPO_4$:Dy^{3+}, Ce^{3+}. *Journal of Luminescence*, **134**, 649-656.

[5] Gheorghe, C., Lupei, A., Voicu, F.M. and Tiseanu, C. (2014) Emission Properties and Site Occupation of Sm^{3+} Ion Doped Lu_2O_3 Translucent Ceramics. *Journal of Alloys and Compounds*, **588**, 388-393.

[6] Li, Y.-C., Chang, Y.-H., Lin, Y.-F., *et al.* (2007) Synthesis and Luminescent Properties of Ln^{3+} (Eu^{3+}, Sm^{3+}, Dy^{3+})-Doped Lanthanum Aluminum Germanate $LaAlGe_2O_7$ Phosphors. *Journal of Alloys and Compounds*, **439**, 367-375.

[7] Shinde, K.N., Dhoble, S.J. and Kumar, A. (2011) Combustion synthesis of Ce^{3+}, Eu^{3+} and Dy^{3+} Activated $NaCaPO_4$ Phosphors. *Journal of Rare Earths*, **29**, 527-535.

[8] Navarro, E., Rodríguez, G., Guzmán-Mendoza, J., García-Hipólito, M. and Falcony, C. (2013) Photoluminescence Response of HfO_2:Eu^{3+} Obtained by Hydrothermal Route. *Open Journal of Synthesis Theory and Applications*, **2**, 73-77. https://doi.org/10.4236/ojsta.2013.22009

[9] Huang, J., Zhou, L., Pang, Q., Gong, F., Sun, J. and Wang, W. (2009) Photoluminescence Properties of a Novel Phosphor CaB_2O_4:Eu^{3+} under UV Excitation. *Luminescence*, **24**, 363-366. https://doi.org/10.1002/bio.1116

[10] Jin, C., Ma, H., Liu, Q., Li, X. and Liu, P. (2014) Photoluminescence Properties of the High-Brightness Eu(3+)-Doped $KNaCa_2(PO_4)_2$ Phosphors. *Spectrochimica Acta A Molecular Biomolecular Spectroscopy*, **25**, 767-771.

[11] Chawla, S., Kumar, N. and Chander, H. (2009) Broad Yellow Orange Emission from $SrAl_2O_4$:Pr^{3+} Phosphor with Blue Excitation for Application to White LEDs. *Journal of Luminescence*, **129**, 114-118.

[12] Van den Eeckhout, K., Smet, P.F. and Poelman, D. (2010) Persistent Luminescence in Eu^{2+}-Doped Compounds: A Review. *Materials*, **3**, 2536-2566. https://doi.org/10.3390/ma3042536

[13] Van den Eeckhout, K., Poelman, D. and Smet, P.F. (2013) Persistent Luminescence in Non-Eu^{2+}-Doped Compounds: A Review. *Materials*, **6**, 2789-2818. https://doi.org/10.3390/ma6072789

[14] Zhao, L.S., Liu, J., Wu, Z.C. and Kuang, S.P. (2012) Optimized Photoluminescence of SrB_2O_4:Eu^{3+} Red-Emitting Phosphor by Charge Compensation. *Spectrochimica Acta Part A*: *Molecular and Biomolecular Spectroscopy*, **87**, 228-231.

[15] Rivera, T., Furetta, C., Azorín, J., Barrera, M. and Soto, A.M. (2007) Thermoluminescence (TL) of Europium-Doped ZrO_2 Obtained by Sol-Gel Method. *Radiation Effects and Defect in Solids*, **162**, 379-383. https://doi.org/10.1080/10420150601135282

[16] Głuchowski, P., Stręk, W., Lastusaari, M. and Hölsä, J. (2015) Optically Stimulated Persistent Luminescence of Europium-Doped LaAlO₃ Nanocrystals. *Physics Chemistry Chemical Physics*, **17**, 17246-17252. https://doi.org/10.1039/C5CP00234F

[17] Dhari, A., Horchani-Nifer, K., Benedetti, A., Enrichi, F. and Ferid, M. (2012) Combustion Synthesis and Photoluminescence of Eu³⁺ Doped LaAlO₃ Nanophosphors. *Optical Materials*, **34**, 1742-1746.

[18] Kaur, J., Singh, D., Dubey, V., Suryarana, N.S., Paraniha, Y. and Jha, P. (2014) Review of the Synthesis, Characterization, and Properties of LaAlO₃ Phosphors. *Research on Chemical Intermediates*, **40**, 2737-2771. https://doi.org/10.1007/s11164-013-1126-z

[19] Chen, B., Yu, J. and Liang, X. (2011) LaAlO₃ Hollow Spheres: Synthesis and Luminescence Properties. *American Chemical Society*, **27**, 11654-11659.

[20] Oliveira, V.H., Khaidukov, N.M., Silva, E.C. and Faria, L.O. (2011) Study of TL Properties of LaAlO₃:Ce,Dy Crystals for UV Dosimetry. *Radiation Measurements*, **46**, 1173-1175.

[21] Singh, V., Watanabe, S., Gundu Rao, T.K., Chubaci, J.F.D. and Kwak, H.-Y. (2011) Characterization, Photoluminescence, Thermally Stimulated Luminescence and Electron Spin Resonance Studies of Eu³⁺ Doped LaAlO₃ Phosphor. *Solid State Sciences*, **13**, 66-71.

[22] Berchmans, L.J., Angappan, S., Visuvasam, A. and Ranjith Kumar, K.B. (2008) Preparation and Characterization of LaAlO₃. *Material Chemical Physics*, **109**, 113-118.

[23] Mendoza-Mendoza, E., Padmasree, P.K., Montemayor, S.M. and Fuentes, A.F. (2012) Molten Salts Synthesis and Electrical Properties of Sr- and/or Mg-Doped Perovskite-Type LaAlO₃ Powders. *Journal of Materials Science*, **47**, 6076-6085. https://doi.org/10.1007/s10853-012-6520-1

[24] Mendoza-Mendoza, E., Montemayor, S.M., Escalante-García, J.I. and Fuentes, A.F. (2012) A "Green Chemistry" Approach to the Synthesis of Rare-Earth Aluminates: Perovskite-Type LaAlO₃ Nanoparticles in Molten Nitrates. *Journal of American Ceramics Society*, **95**, 1276-1283. https://doi.org/10.1111/j.1551-2916.2011.05043.x

[25] Koc, N.S., Oksuzomer, F., Yasar, E., Akturk, S. and Gurkaynak, M.A. (2006) Affect Sol-Gel Modifications on Formation and Morphology of Nanocrystalline Lanthanum Aluminate. *Material Research Bulletin*, **41**, 2291-2297.

[26] Rivera, T., Olvera, L., Azorín, J., Sosa, R., Soto, A.M., Barrera, M. and Furetta, C. (2006) Preparation of Luminescent Nanocrystals Started from Amorphous Zirconia Prepared by Sol-Gel Technique. *Radiation Effects and Defects in Solids*, **161**, 91-100. https://doi.org/10.1080/10420150600615847

[27] Pechini, M.P. (1967) Method of Preparing Lead and Alkaline Earth Titanates and Niobates and Coating Method Using the Same to Form a Capacitor. United States Patent Office, Patent 3,330,697.

[28] Hernández, M.T. and González, M. (2002) Synthesis of Resins as Alpha-Alumina Precursors by the Pechini Method Using Microwave and Infrared Heating. *Journal of the European Ceramic Society*, **22**, 2861-2868.

[29] Huízar-Félix, A.M., Hernández, T., de la Parra, S., Ibarra, J. and Kharisov, B. (2012) Sol-Gel Based Pechini Method Synthesis and Characterization of Sm₁₋ₓCaₓFeO₃. Perovskite 0.1 ≤ *x* ≤ 0.5. *Powder Technology*, **229**, 290-293.

[30] Pagonis, V., Kitis, G. and Furetta, C. (2005) Numerical and Practical Exercises in Thermoluminescence. Springer, Berlin, 23.

[31] Chen, R. (1969) On the Calculation of Activation Energies and Frequency Factors

from Glow Curves. *Journal of Applied Physics*, **40**, 570-585.
https://doi.org/10.1063/1.1657437

[32] Rivera-Montalvo, T., Morales-Hernandez, A., Barrera-Angeles, A.A., Alvarez-Romero, R., Falcony, C. and Zarate-Medina, J. (2017) Modified Pechini's Method to Prepare LaAlO$_3$:RE Thermoluminescent Materials. *Radiation Physics and Chemistry*, in press.

[33] Boronat, C., Rivera, T., Garcia-Guinea, J. and Correcher, V. (2017) Cathodoluminescence Emission of REE (Dy, Pr and Eu) Doped La AlO$_3$ Phosphors. *Radiation Physics and Chemistry*, **130**, 236-242.